Supporting Information

Visible-light-driven Dry Reforming of Methane Using Semiconductor Supported Catalyst

Yohei Cho,[a] Shusaku Shoji,[a] Akira Yamaguchi,[a] Takuya Hoshina,[a] Takeshi Fujita,[b] Hideki Abe,[c] and Masahiro Miyauchi[*a]

[a] *Department of Materials Science and Engineering, Tokyo Institute of Technology, 2-12-1 Ookayama, Meguro-ku, Tokyo 152-8552, Japan*

[b] *School of Environmental Science and Engineering, Kochi University of Technology, 185 Miyanokuchi, Tosayamada, Kami, Kochi 7 782-8502, Japan*

[c] *National Institute for Materials Science, 1-1 Namiki, Tsukuba, Ibaraki 305-0044, Japan*

Contents

1. Experimental

1.1. Experimental method

The yellow TaON powder was prepared by nitridizing Ta_2O_5 (WAKO Ltd.) at 850 ℃ for 15 h under an ammonia flow of 20 mL/min. After heat treatment, rhodium chloride trihydrate was added to TaON with a weight ratio of Rh/TaON=5/100 and dissolved in distilled water. The solution was poured into a polytetrafluoroethylene vessel and was hydrothermally treated at 200 ℃ for 12 h. After hydrothermal treatment, the sample was washed by water and dried at 100 ℃ until the sample was completely dried. Before the catalytic performance test, the sample was reduced at 500 ℃ under the reaction conditions of $Ar/CH_4/CO_2$=98/1/1 for 1 hour. Red Ta_3N_5 powder was purchased from Kojundo Chemical Lab. Co., Ltd.; Rh particles were deposited onto Ta_3N_5 powder in the same manner described for TaON. We also investigated other methods for Rh loading (in addition to hydrothermal treatment) to achieve high DRM activity. Detailed procedures for the other methods are described in the Supporting Information (Section 3, process optimization). Hydrothermal treatment was determined to be the best method to prepare Rh/TaON with high DRM activity.

Characterization was conducted using X-ray diffraction (Rigaku, Smartlab), TEM (JEOL Ltd., JEM-2010), UV-vis with a diffuse reflection unit (JASCO Corporation, V-670), and TG-DTA (NETZSCH, STA2500 Regulus). The XRD scan rate was 5 ゚/min. The acceleration voltage of TEM was 200 kV. TG-DTA analysis was conducted under 20 mL/min air flow with a 20 ℃/min temperature ramp to 1000 ℃. For ICP analysis, Rh/TaON powder was dissolved into the mixture of nitrate acid and sulfuric acid together with NH_4F solution. Subsequently, the sample went through pressurized acid decomposition treatment for 20 h, where temperature was 220 ℃.

Catalytic performance was evaluated using a flow reactor described in Scheme S1. The composition of feed gas was $Ar/CH_4/CO_2$=98/1/1 and the flow rate was 10 mL/min. To evaluate temperature dependence, the temperature was increased at 20 ℃/min and maintained at each measuring temperature for 2.5 min.

1.2. Evaluation system and condition
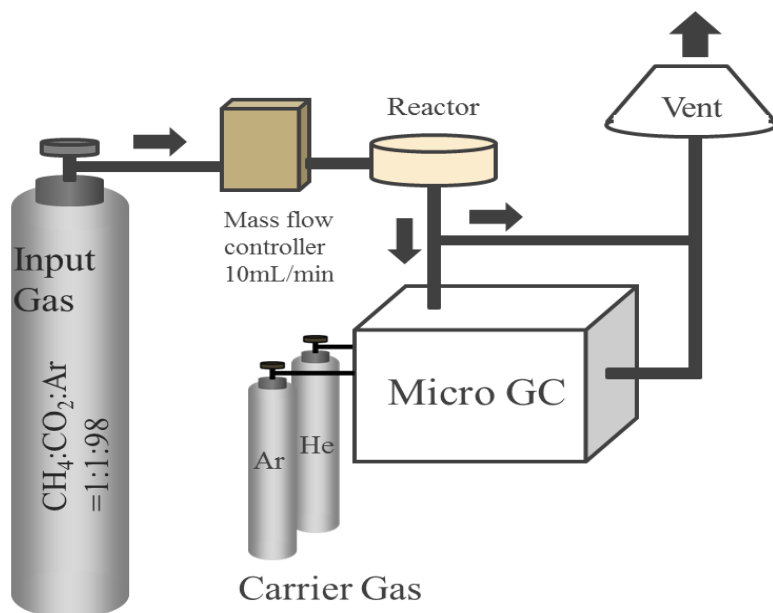
Scheme S1. Experimental setup for the evaluation of the catalytic activity.
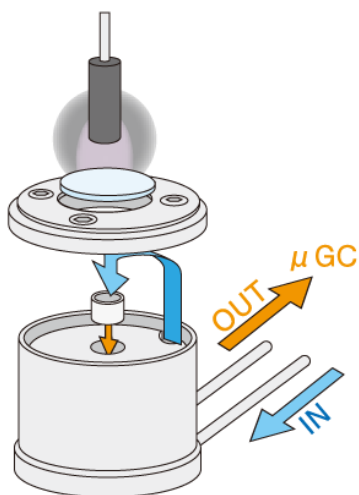
Scheme S2 The schematic illustration of a reactor for DRM reaction in the present study.
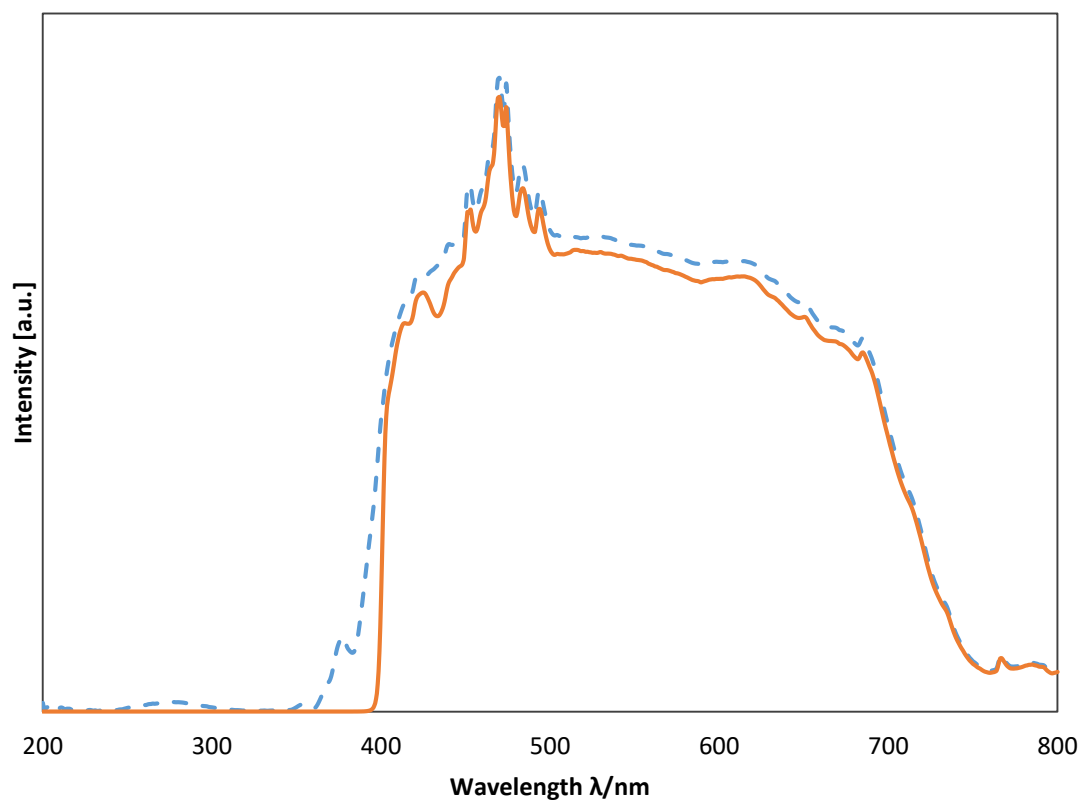
1. 3. Light source for photocatalysis test

Fig. S1 The spectrum of visible light source used in the experiment (orange) and the original Xe light source without an UV cutoff filter (blue dash line). The integrated light intensity with cutoff filter was 2.54 W/cm^2 measured by a spectro-radiometer.

1.4. Calculation of the consumption rate of CH_4 and CO_2, the rate of H_2 production, and the yield of H_2

$$\text{Consumption rate } [\mu mol/min]$$
$$= \{(\text{Concentration of input gas})[ppm]$$
$$- (\text{Concentration of output gas})[ppm]\} * \frac{9.0 \ [\mu mol/min]}{20000 \ [ppm]}$$

$$\text{Rate of } H_2 \text{ production } (r_{H_2}) \ [\mu mol/min]$$
$$= \text{Concentration } [ppm] * \frac{9.0 \ [\mu mol/min]}{20000 \ [ppm]}$$

$$\text{Yield } [\%] = \frac{\text{Concentration of output gas } [ppm]}{\text{Concentration of input gas } [ppm]} \times 100 \ [\%]$$

1.5. Calculation of turnover number (TON)

$$\text{TON} = \frac{\text{Generated } H_2 \ [mol]}{\text{Rh } [mol]}$$

1.6. Effect of temperature gradient in a reactor

As the recent study suggested the effect of light-induced temperature gradient between the top-surface and bottom-surface of a catalyst bed.[1] However, in the previous study,[2] Jiang et al. put TaC, which is known for its high photo-thermal conversion efficiency, onto Rh catalyst to investigate the effect of temperature gradient. Then, the temperature gradient did not affect the catalytic activity. In the present case, we used the same reactor under light irradiation, thus, the double-temperature zone would not cause large effect on our catalyst activity.
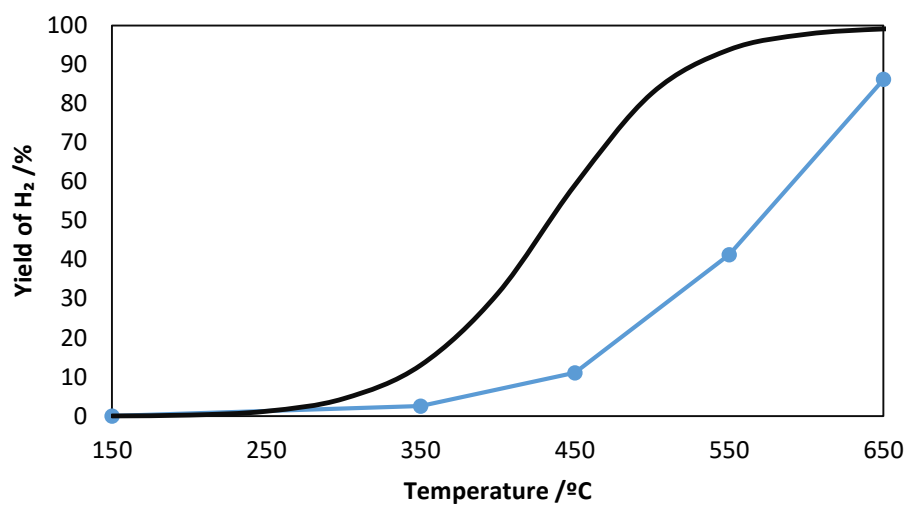
2. Catalytic activity of Rh/SiO$_2$

Fig. S2 H$_2$ production yields of Rh/SiO$_2$ under dark condition.

3. Process optimization

Rh nanoparticles were loaded on TaON using three methods, *i. e.* impregnation, hydrothermal, and photo-deposition methods. For all methods, a solution of TaON and rhodium chloride trihydrate in distilled water was used. For the impregnation method, the solution was kept at 100 °C and stirred at 200 rpm. For the hydrothermal method, the solution was treated at 200 °C for 12 h. For photo-deposition, the solution was irradiated with a Xe lamp with stirring at 200 rpm. For all methods, the sample was collected by centrifugation and dried. Before photocatalysis evaluation, all samples were treated at 500 °C under DRM conditions to reduce the Rh ions to the metal.

Among these Rh deposition methods, particles prepared by the hydrothermal method achieved the highest DRM activity under visible light irradiation, as shown in Fig. S3. The reason can be explained by the significant difference in the size distribution of Rh particles (see Fig. S8). The small and uniform Rh nanoparticles on TaON prepared by the hydrothermal method increase the number of active site and enhance the electron injection efficiency at the interface.
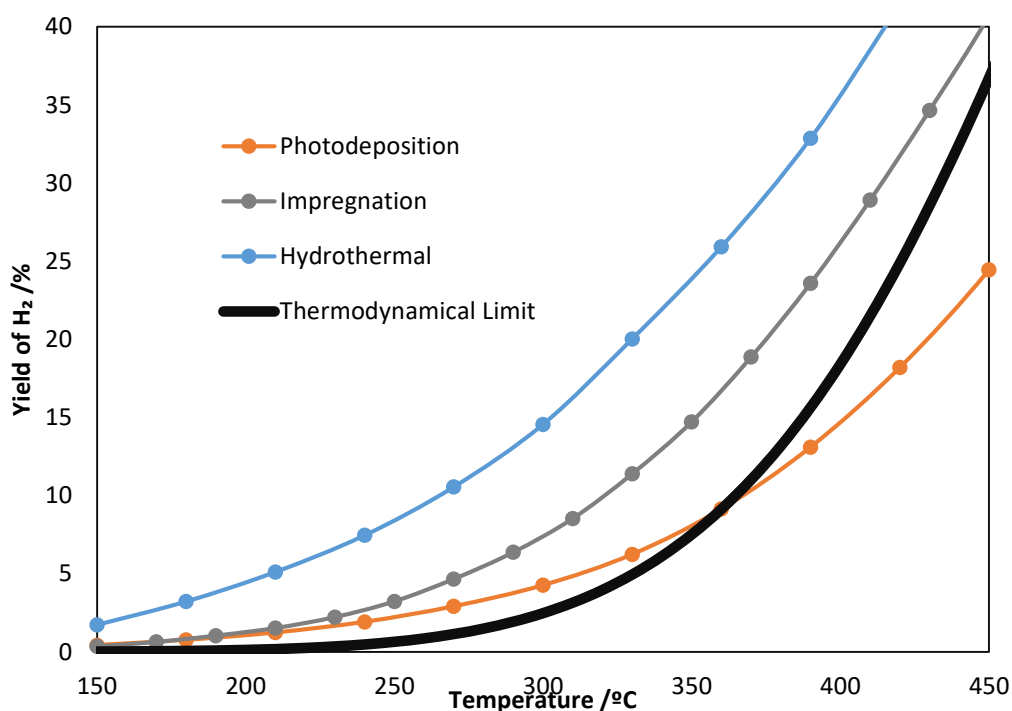

Fig. S3 H_2 production yields under light irradiation for the samples prepared by different methods.
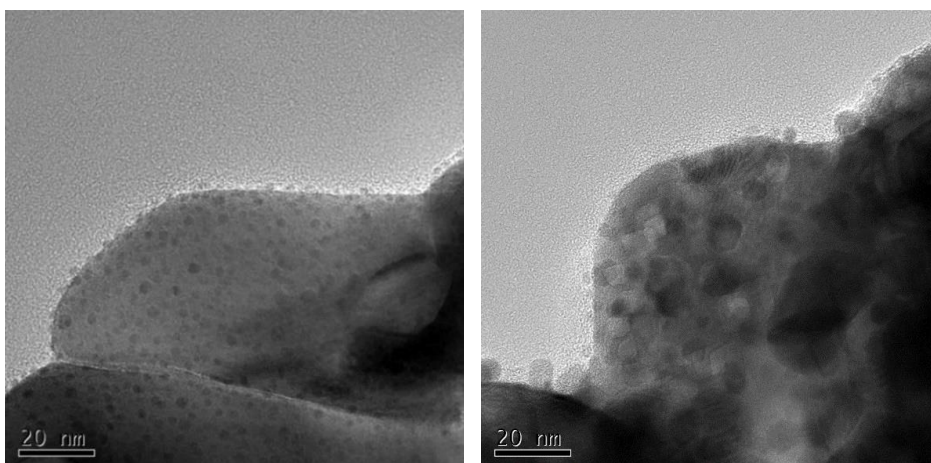
Fig. S4 TEM images of Rh/TaON prepared by hydrothermal method (left) and impregnation method (right).
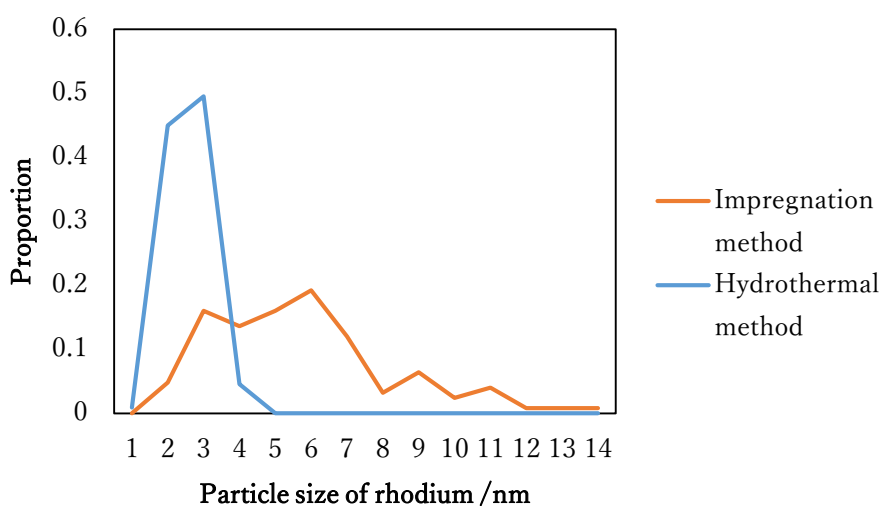

Fig. S5 Size distributions of Rh particles on TaON prepared by impregnation method (orange) and hydrothermal method (blue).

We have statistically estimated the size distribution of Rh nano-particles on the basis of TEM images shown in Fig. S8. In the case of impregnation method, we have measured the size of 128 particles, while in the case of hydrothermal method, we observed 111 particles. The small and uniform Rh nanoparticles on TaON were seen in the hydrothermally prepared sample as compared to the sample prepared by an impregnation method. The hydrothermal process increased the number of active site and would promote the efficient carrier transport at the interface of Rh/TaON.

8

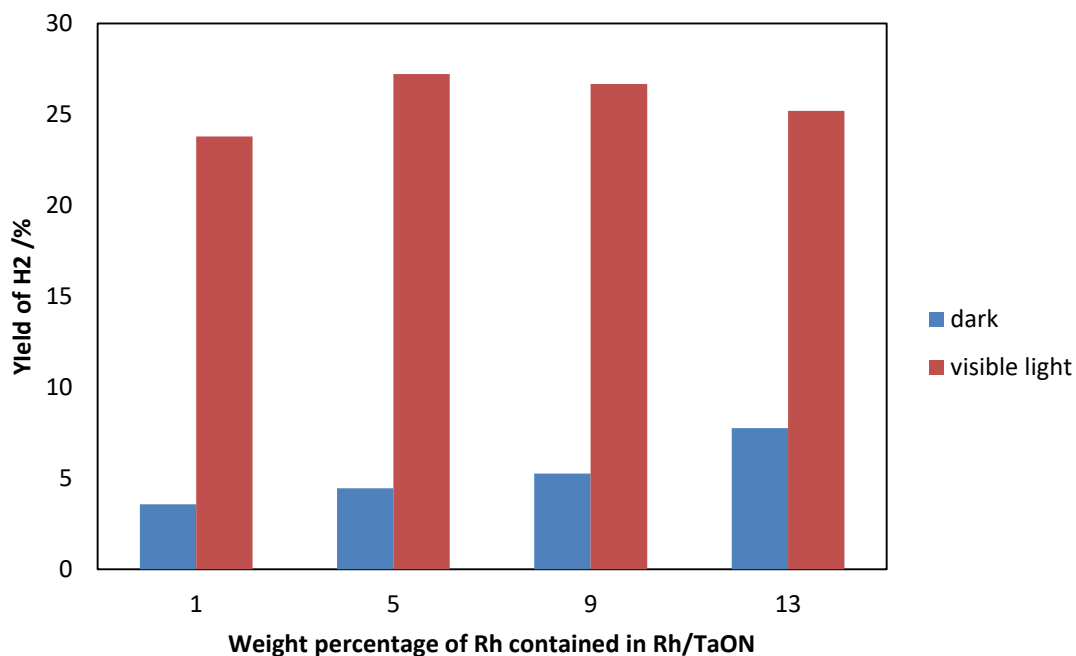## 4. Optimization of the rhodium loading amount

Fig. S6 The performance of Rh/TaON with different weight percentage of Rh precursor.

Various percentage of Rh (1%, 5%, 9%, 13% of precursor amount) was loaded on TaON and their catalytic and photocatalysis performance was compared. As the content of Rh increased, the yields exhibited monotonic increase under dark condition, whereas the optimum yield at 5 wt% was seen under light irradiation condition. The different trend also suggests that the reaction mechanism under light irradiation is different from that under thermal process. Rh/TaON photocatalysis needs the excitation of TaON, thus the overloading of Rh shadows the light irradiation to TaON and decreases the DRM activity.

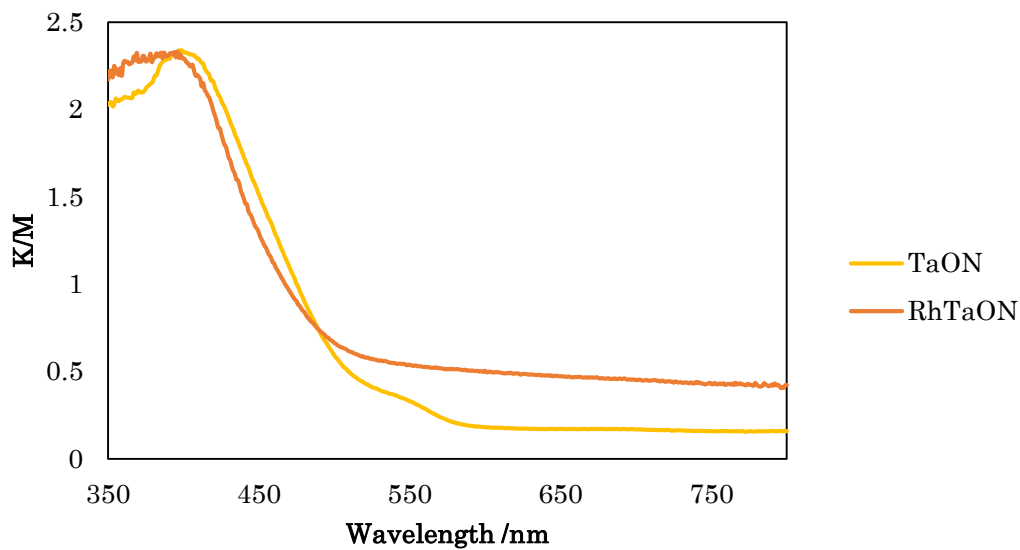5. Optical property (comparison between TaON and Rh/TaON, estimation of bandgap)

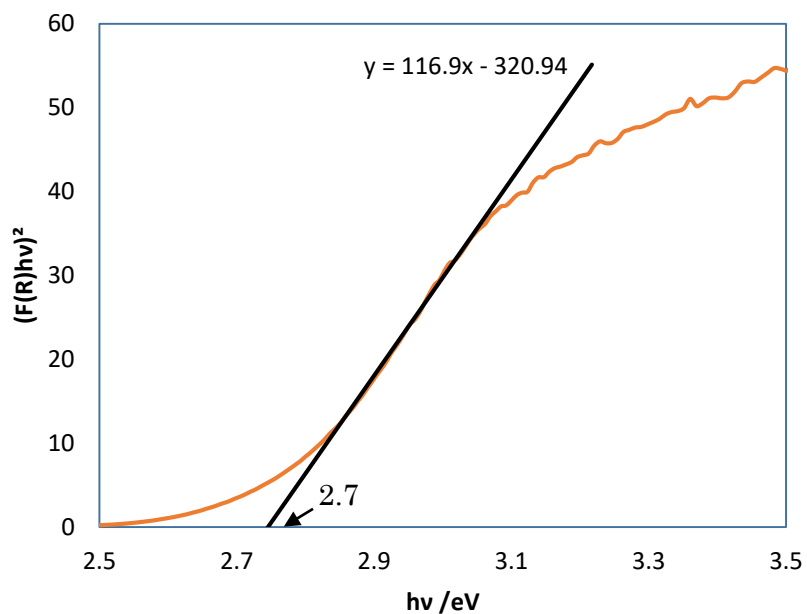Fig. S7 Comparison of UV-vis spectra between TaON and Rh/TaON
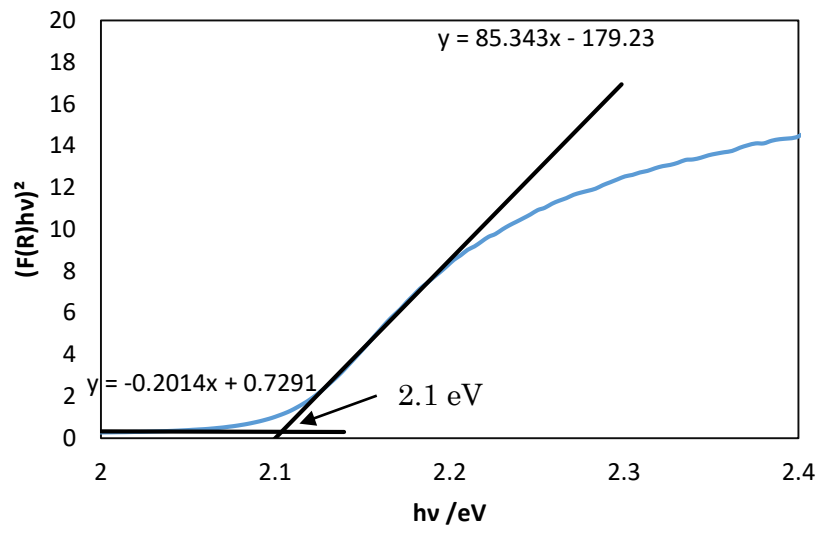

Fig. S8 Tauc plot of TaON

y = 85.343x - 179.23

y = -0.2014x + 0.7291

2.1 eV

(F(R)hv)²

hv /eV

Fig. S9 Tauc plot of Ta₃N₅
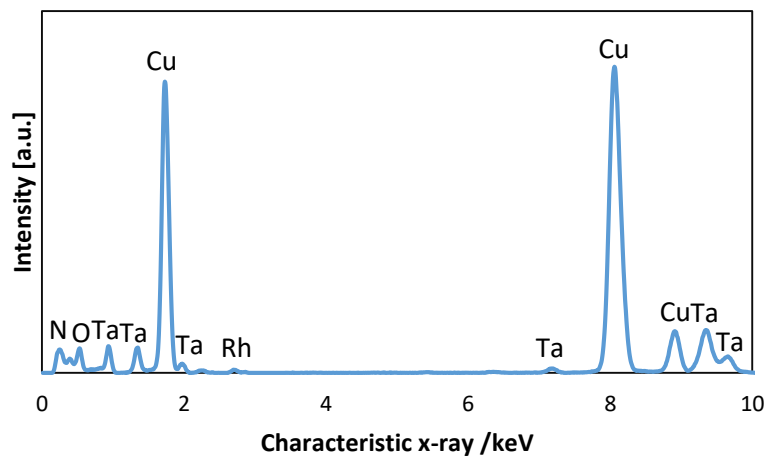
6. EDS, XRD, and XPS analysis on Rh/TaON

Fig. S10 EDS spectrum of Rh/TaON.

Energy dispersive X-ray spectroscopy (EDS) analyses equipped in a TEM apparatus were performed at the spot in Figure 1(c) in the main text. The peaks of Cu are originated from a micro-grid used in TEM analysis.
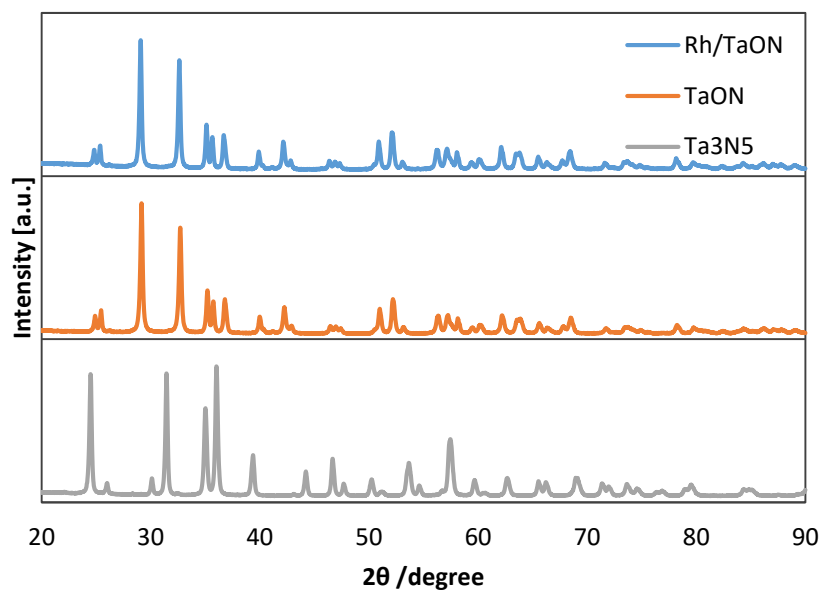
Fig. S11 X-ray diffraction (XRD) patterns of Rh/TaON, TaON and Ta_3N_5

All the peaks of TaON and Ta_3N_5 was assigned to TaON and Ta_3N_5. There was no peak which was assigned to rhodium in Rh/TaON, since the size of the rhodium nanoparticles was so small to be detected by X-ray diffraction.
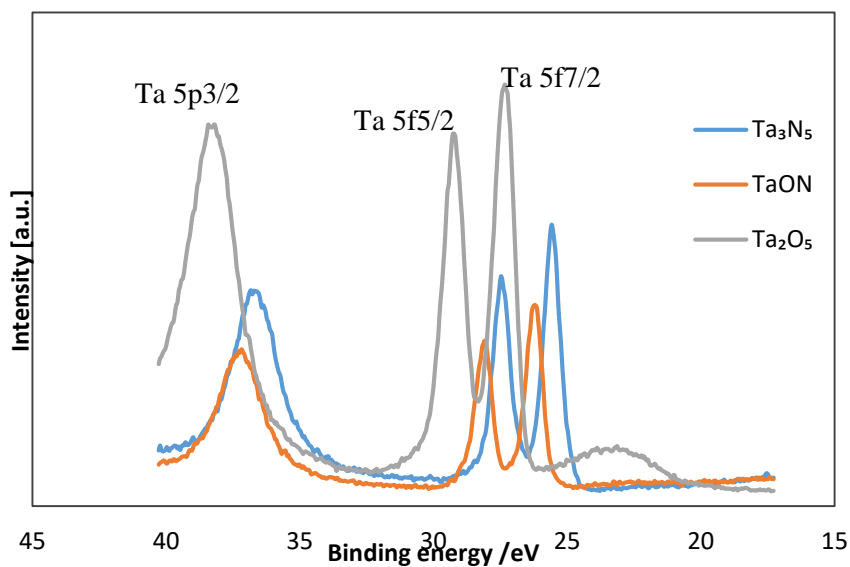

Fig. S12 Hard X-ray photoelectron spectroscopy (HAXPES) analysis on the core level of tantalum (Ta-5p and Ta-5f orbitals).
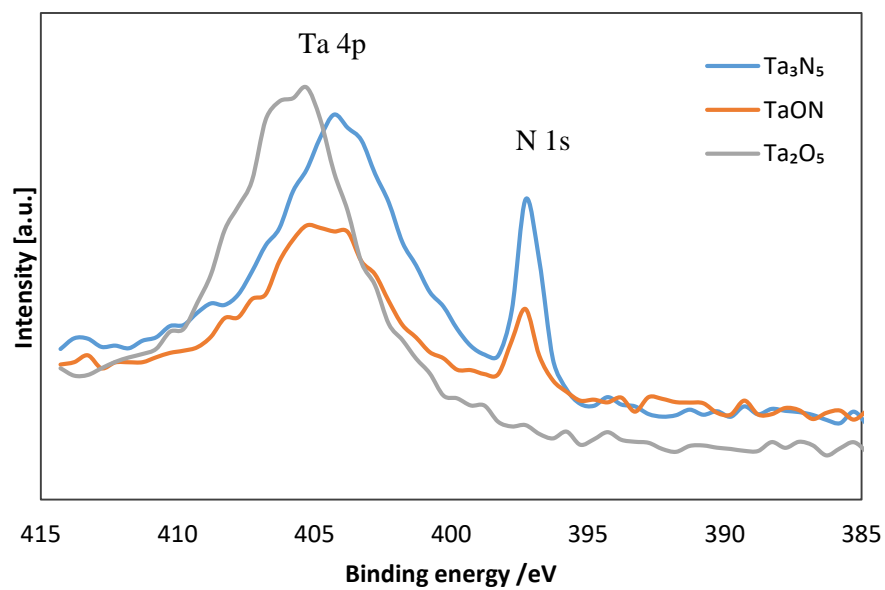
Fig. S13 Hard X-ray photoelectron spectroscopy (HAXPES) analysis for Ta-4p and N-1s.
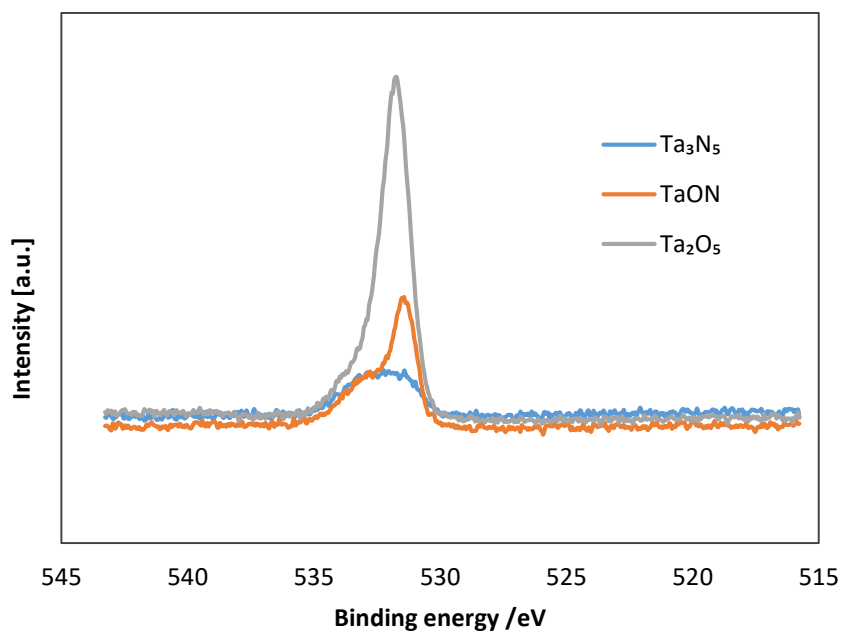

Fig. S14 Hard X-ray photoelectron spectroscopy (HAXPES) analysis for O-2p.

7. DRM activities for Rh/TaON and Rh/Ta$_3$N$_5$ under dark condition, and TEM image of Rh/Ta$_3$N$_5$
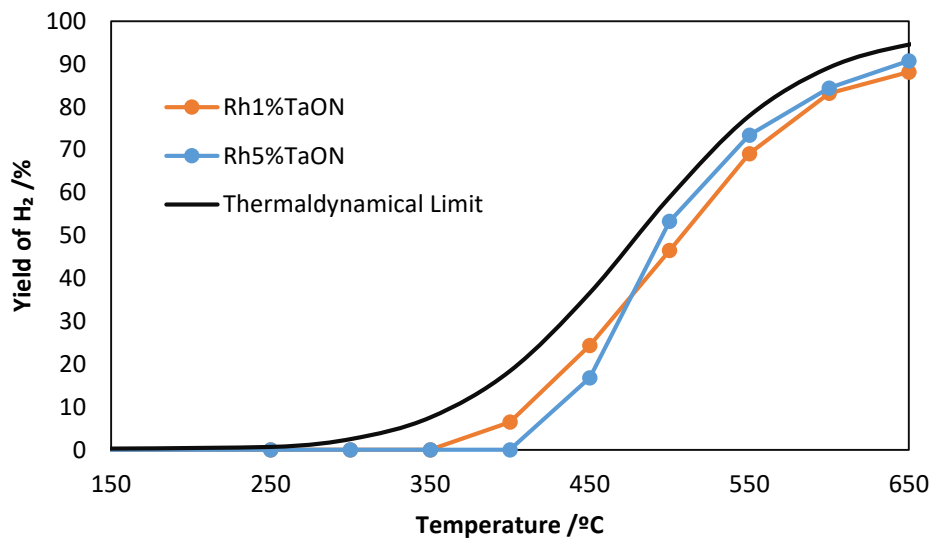

Fig. S15 H$_2$ production yields under dark condition for the samples with different amount of rhodium loading on TaON.
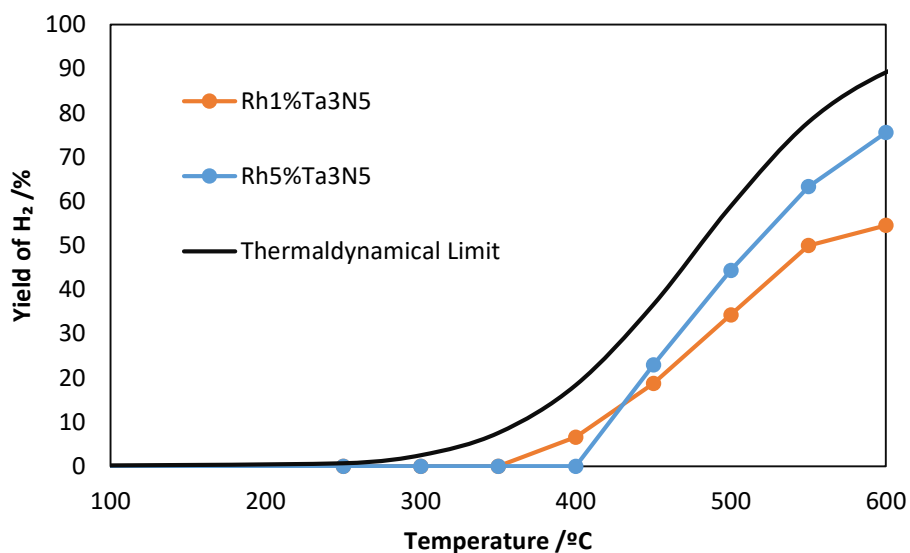

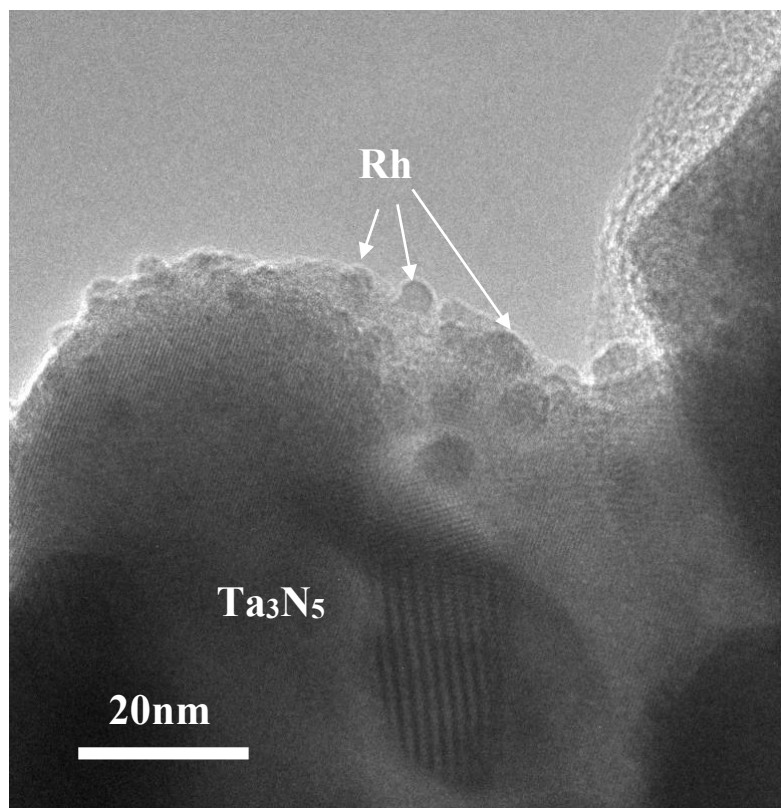Fig. S16 H$_2$ production yields under dark condition for the samples with different amount of rhodium loading on Ta$_3$N$_5$.

Fig. S17 TEM image of Rh/Ta₃N₅.

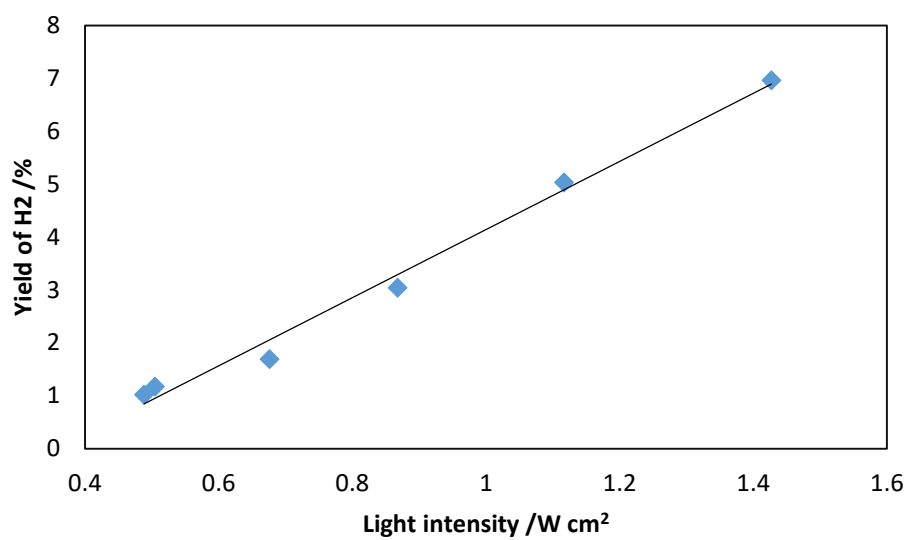8. Light intensity dependence on photocatalytic activiity

Fig. S18 Light intensity dependence on the photocatalytic DRM activity of Rh/TaON.

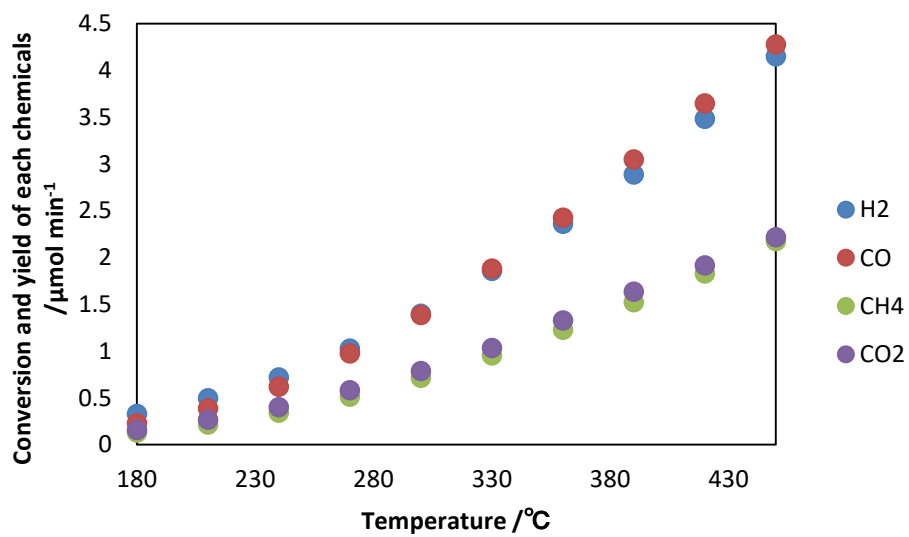9. Conversion of CH$_4$, CO$_2$ and yield of H$_2$, CO for Rh/TaON as a fuction of reaction temperature

Fig. S19 Conversion of CH$_4$, CO$_2$ and yield of H$_2$, CO for Rh/TaON.

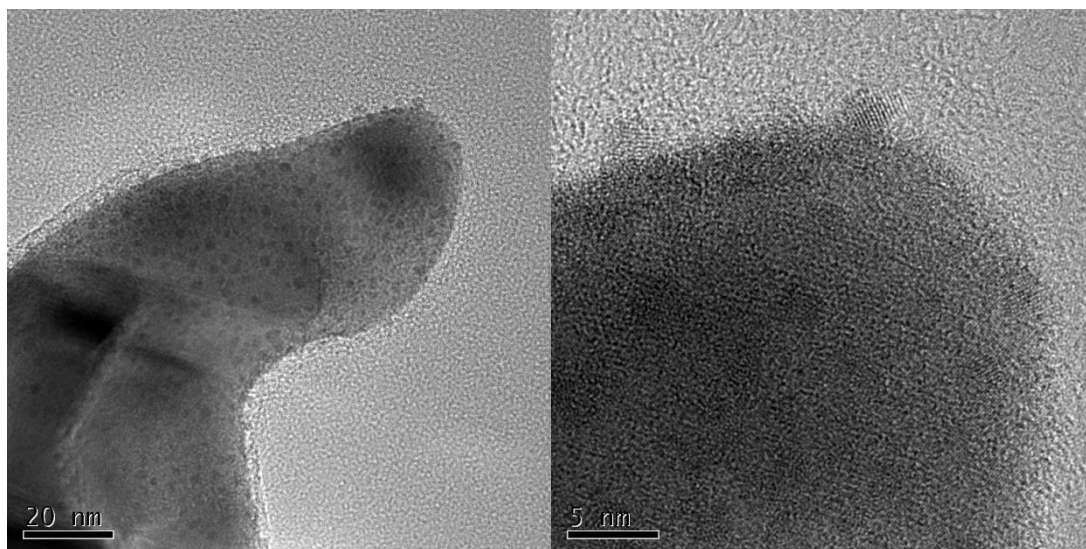## 10. TEM images of Rh/TaON after long time DRM reaction

Fig. S20 TEM images of Rh/TaON after the DRM reaction under light irradiation for 8h.

11. Experimental procedure for comparison between light irradiated condition and the dark condition at the same surface temperature
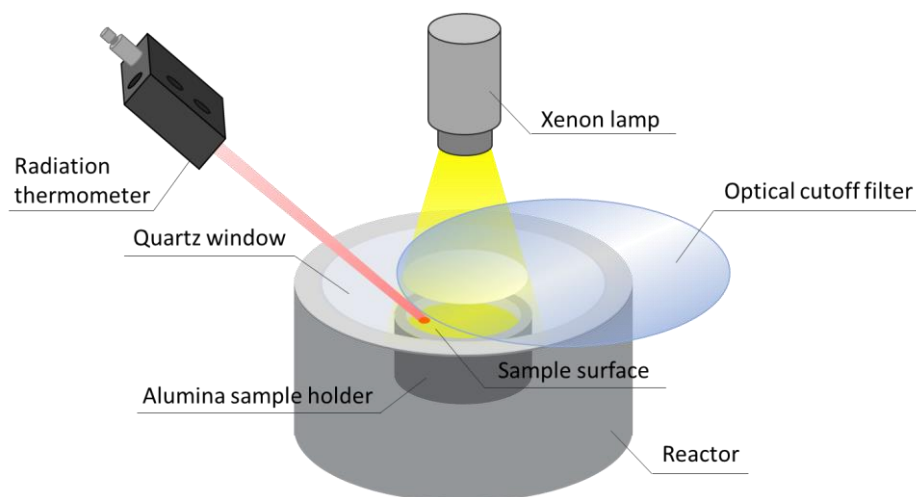

Fig. S21 The method for measuring surface temperature

Table S1 The surface temperature and the reactor (bulk) temperature measured by a radiation thermometer for the experiment of Fig. 3(a) in the main text.

	Light on	Dark
Reactor (bulk) temperature /°C	210	316
Surface temperature /°C	316	316

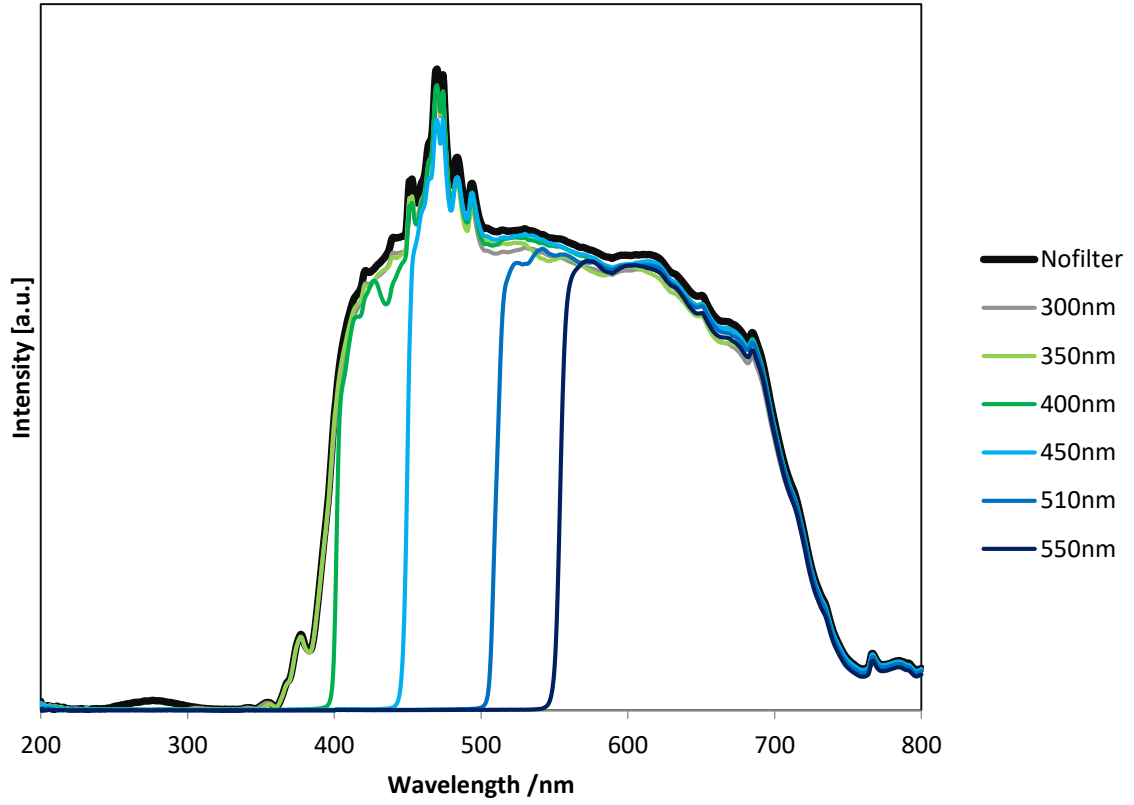12. The spectrum using cutoff filters for action spectrum analysis

Fig. S22 The spectra of various light source using cutoff filters

13. Surface temperature measured while irradiating Xe lamp with various cutoff filter
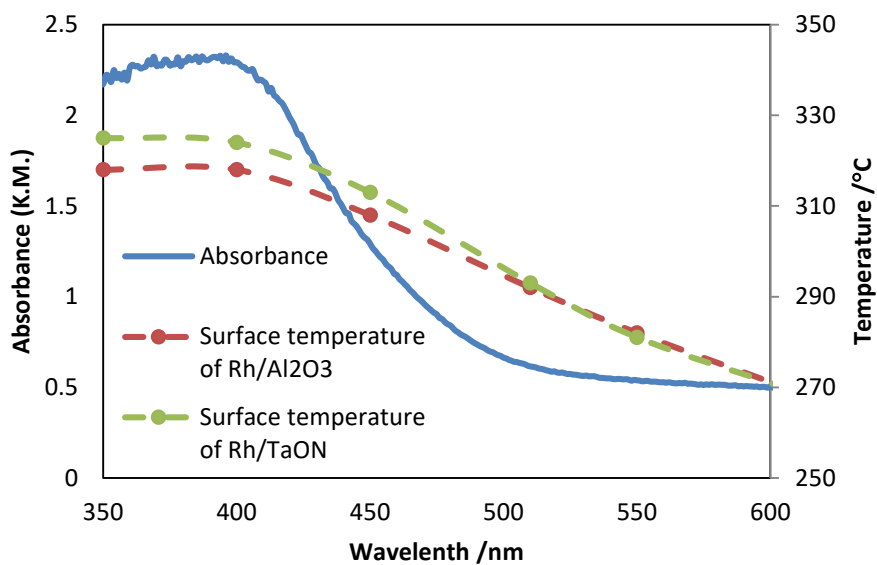

Fig. 23 Overlay of absorbance of Rh/TaON, surface temperature of Rh/TaON and Rh/Al$_2$O$_3$

References in Supporting Information

1.   X. Li, X. Zhang, H. O. Everitt and J. Liu, *Nano Letters*, 2019, **19**, 1706-1711.
2.   H. Jiang, X. Peng, A. Yamaguchi, T. Fujita, H. Abe and M. Miyauchi, *Chemical Communications*, 2019, **55**, 13765-13768.